

## Lifetime measurements on collector optics from Xe and Sn extreme ultraviolet sources

S. N. Srivastava,<sup>a)</sup> K. C. Thompson, E. L. Antonsen, H. Qiu, J. B. Spencer, D. Papke, and D. N. Ruzic

*Center for Plasma Material Interactions, University of Illinois, 103 S. Goodwin Ave., Urbana, Illinois 61801*

(Received 14 March 2007; accepted 4 June 2007; published online 19 July 2007)

Next generation lithography to fabricate smaller and faster chips will use extreme ultraviolet (EUV) light sources with emission at 13.5 nm. A challenging problem in the development of this technology is the lifetime of collector optics. Mirror surfaces are subjected to harsh debris fluxes of plasma in the form of ions, neutrals, and other radiation, which can damage the surface and degrade reflectivity. This manuscript presents the measurement of debris ion fluxes and energies in absolute units from Xe and Sn EUV sources using a spherical sector ion energy analyzer. Experimentally measured erosion on Xe exposed samples is in good agreement with predicted erosion. This result allows prediction of erosion using measured ion fluxes in experiment. Collector optic lifetime is then calculated for Xe and Sn sources without debris mitigation. Lifetime is predicted as 6 h for Xe EUV sources and 34 h for Sn EUV sources. This result allows calculation of expected collector optic lifetimes, which can be an important tool in optimizing source operation for high volume manufacturing. © 2007 American Institute of Physics. [DOI: 10.1063/1.2756525]

### INTRODUCTION

The use of extreme ultraviolet (EUV) light in lithography is a promising method for high volume commercial manufacturing (HVM) of sub-100-nm feature-size transistors in integrated circuits. EUV light at 13.5 nm was selected for research in the 1990s by the Extreme Ultraviolet Limited Liability Corporation (EUV LLC) Consortium, founded by Intel, Motorola, and AMD. Printing of sub-100-nm features was demonstrated in 2002,<sup>1</sup> leading to a wide recognition of the feasibility of EUV lithography.

Li, Sn, and Xe are known to generate significant amounts of light in the EUV range when excited in laser- or discharge-produced plasmas.<sup>2</sup> These plasmas create the high level of ionization required to generate 13.5 nm light. For Xe, this wavelength is emitted from Xe<sup>10+</sup>, whereas for Sn, multiple ion species from Sn<sup>8+</sup> to Sn<sup>12+</sup> are responsible for EUV emission in 13.5 nm radiation bandwidth. Implementation of this technology is hindered by the amount of debris typically generated in EUV emitting plasmas in the form of ions, electrons, neutrals, and solid matter. These particles can damage the surfaces of nearby mirror optics, degrading their useful lifetime. For this reason, several methods for characterizing and mitigating the debris from pinch plasmas are explored. Use of a collimating foil trap along with a neutral gas curtain<sup>3</sup> shows considerable success. Other experiments performed to demonstrate mitigation include the manipulation of magnetic<sup>4</sup> and electric<sup>5</sup> fields, as well as the introduction of low-mass molecules into the fuel.<sup>6</sup> In a high volume manufacturing setting, it is economically undesirable to perform a frequent maintenance on clean-room equipment due to the amount of time that production must be halted. Any combination of light source and optics system that will result

in a useful lifetime is dependent on the optics materials used, the location of the optics, and the debris emitted from the source. In order to know the feasibility of any combined source and optics setup, this lifetime must be calculated.

Methods of ion energy measurement, particle detection, debris studies and mitigation on Xe and Sn based sources, erosion of extreme ultraviolet lithography (EUVL) candidate collector mirror materials, etc., have been studied by several researchers.<sup>4,5,7-14</sup> Hansson *et al.*<sup>7</sup> reported the importance of measurements of ion emission characteristics. They also estimated the ion energies using a Faraday cup in time-of-flight analysis. However, they could not obtain the fluxes in absolute units as the average charge reaching the Faraday cup was unknown. Takenoshita *et al.*<sup>8</sup> have measured ions using Faraday cup, electrostatic ion energy analyzer, and Thompson parabola ion spectrometer. Using the ion energy analyzer they measured ions up to 5+ in the case of a Sn source. They also reported particle detection using witness plates, which were analyzed through several material characterization techniques.

Research conducted to this point lacks a systematic investigation of ion flux and energy in absolute units. This is also a need for lifetime calculations based on experimental data such that source suppliers and mirror suppliers can optimize performance of products used in the manufacturing tools. Experiments done at the Center of Plasma Material Interactions (CPMI) characterize ionic debris emitted from a commercial z-pinch source fueled by Xe and SnCl<sub>4</sub> in absolute units. Ion debris from both sources are compared for dominant fuel ions as well as other ions generated in the plasma. Several EUV compatible mirror samples are exposed to the plasma at a distance similar to that of a typical optical collector setup. Surface analysis is performed both before and after the exposure to explore the effect of debris on the

<sup>a)</sup>Electronic mail: sns@uiuc.edu

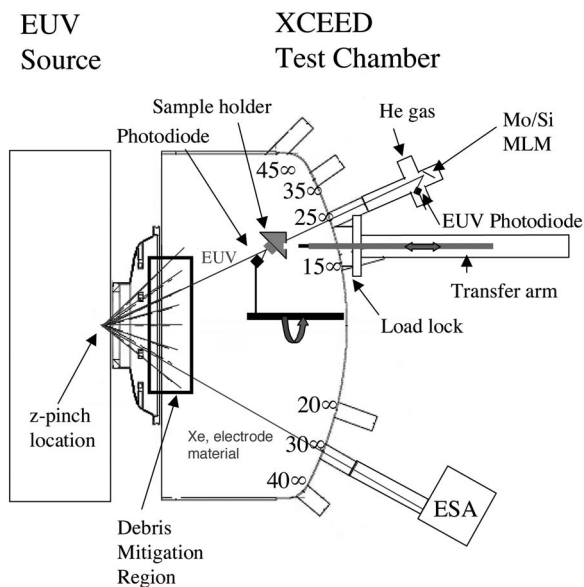


FIG. 1. The XCEED test chamber allows diagnostic access at 5° increments from 15° to 45° off the z-pinch axis.

optical materials. Using this data, an estimate of the optics lifetime under HVM conditions is calculated.

## EXPERIMENT

An XTREME Technologies GmbH (Ref. 15) XTS 13–35 EUV light source is used to produce 13.5 nm light; the source is fueled by either Xe or SnCl<sub>4</sub>. The fuel gas enters the pinch area after having been preionized. Next, the source compresses the gas into a cylinder of approximately 1 mm length × 0.5 mm width, causing the gas to become highly ionized and emit 13.5 nm light. Out of band radiation is also emitted from the pinch, as well as electrons, ions, and neutral atoms.

Attached to the EUV source, the XTREME commercial EUV emission diagnostic (XCEED) chamber provides line-of-sight access to the pinch from a variety of angles (Fig. 1). A range of seven ports allows diagnostics to be attached at multiple angles to measure ion debris spectra and EUV light. Further, four ports allow real-time unloading and reloading of samples during exposure tests. A pair of Osaka<sup>16</sup> MT-series turbomolecular pumps allows an achievable base pressure of  $1 \times 10^{-7}$  Torr. A more detailed description of the chamber is given in Thompson *et al.*<sup>3</sup> To measure the 13.5 nm EUV light, an IRD (Ref. 17) Ti/Zr/Si 6/480/50 nm photodiode is utilized. To avoid direct exposure to pinch debris, light is reflected to the photodiode from a 40 Mo/Si bilayer mirror with a 4 nm Si capping layer; the reflectivity of this mirror is 70%. The photodiode setup is housed behind a 2 mm orifice at the 30° port. Helium gas flows into the photodiode housing to protect the mirror from debris.<sup>18</sup>

The ion fluxes are measured using a Comstock<sup>19</sup> AC-902b spherical sector energy analyzer (ESA) fitted with Burle<sup>20</sup> CP-618C dual microchannel plate (MCP) detectors. The ESA uses energy-to-charge ratio to bias for ions and is able to measure singly charged ion energies up to 15 keV, doubly charged up to 30 keV, and so on. The ESA itself is

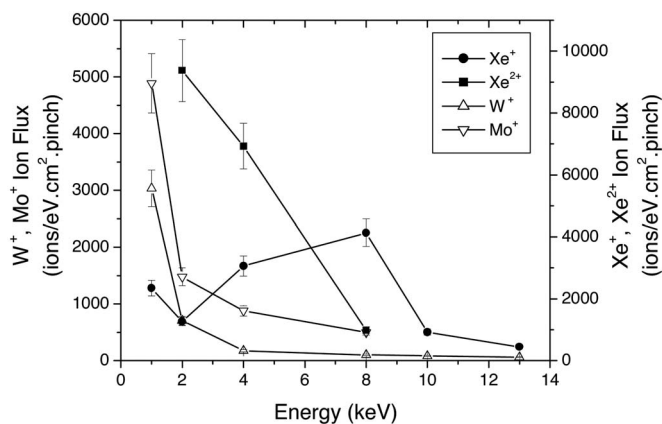


FIG. 2. Ion spectra from Xe-fueled XTS measured with ESA without buffer gas at a distance of 157 cm from the pinch.

situated at the 20° port behind a 2 mm orifice to allow for differential pumping. Use of a bellows in the path to the ESA allows three-dimensional laser alignment to the pinch. A more detailed treatment of the ESA is found in Antonsen *et al.*<sup>21</sup> The MCP signal travels through an Ortec (Ref. 22) 9326 fast preamplifier, after which it is measured by a 1 GHz Agilent<sup>23</sup> Infinium 54832B oscilloscope. The signal itself is a 7 ns wide downward spike; measured signals are accumulated into spectra using the histogram function of the oscilloscope. These spectra can be converted into units of absolute ion flux using calibration curves, which are obtained by aiming an ion gun at the ESA and comparing histogram signals to corresponding Faraday cup signals (a detailed discussion of this calibration is present in Antonsen *et al.*<sup>21</sup>). The 0 μs point on the time scale of the debris spectra is set equal to the point of capacitive discharge of the z pinch. Ion debris is not visible for the entirety of the time scale; noise generated by the pinch interferes with ion signals occurring at times less than 10 μs.

The XCEED source has been upgraded to produce EUV light from Sn ions. This is accomplished by flowing SnCl<sub>4</sub> into the pinch region instead of Xe. Tin gaseous delivery system for the University of Illinois at Urbana-Champaign (UIUC) XTS 13–35 source requires an exhaust system to deal with the toxic by-products of the SnCl<sub>4</sub> breakdown within the source. Delivery of SnCl<sub>4</sub> to the source includes a heated reservoir and heated delivery lines to reduce freezing and blockage of feed lines.

Several samples are exposed to Xe and Sn sources in order to measure the erosion caused by plasma debris. In the case of Xe, samples are exposed for  $10 \times 10^6$  shots at a distance of 56 cm from the pinch location. Due to constraints imposed by exhaust-gas processing, the source with Sn could not be operated for a longer time. Thus to obtain an equal exposure shots in the case of Sn source, the device is operated at higher frequency and samples are moved closer to the pinch. In this way an equivalent flux is achieved in a shorter time of operation.

## RESULTS AND DISCUSSION

Ion debris fluxes are measured from the Xe source as well as the SnCl<sub>4</sub>-fueled z pinch. Figure 2 shows the ion

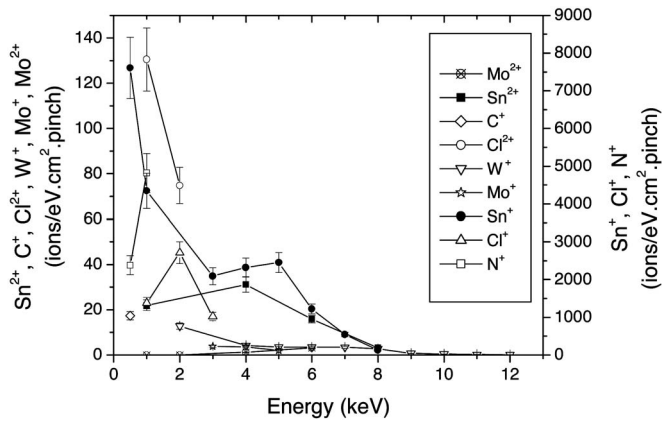


FIG. 3. Ion spectra from Sn-fueled XTS measured with ESA without buffer gas at a distance of 157 cm from the pinch.

spectra of Xe-fueled XTS source in ions/eV cm<sup>2</sup> pinch plotted on the y axis against the ion energies in keV on the x axis. Four different ion species (Xe<sup>+</sup>, Xe<sup>2+</sup>, Mo<sup>+</sup>, and W<sup>+</sup>) are resolved in this measurement. Ion spectra shown in Fig. 2 are measured without buffer gas at 20° from the pinch. Dominant ion species are Xe<sup>+</sup> and Xe<sup>2+</sup>. Xe<sup>+</sup> peaks at 8 keV, whereas Xe<sup>2+</sup> is found mostly at lower energies and the flux decreases at higher energies. Note that after 8 keV, there are no Xe<sup>2+</sup> ions measured, which may be the result of high recombination in the pinch area. Xe<sup>+</sup> is found up to 13 keV, which may include Xe<sup>2+</sup> ions recombined to Xe<sup>+</sup> ions. Tungsten and molybdenum ions are also measured, which are from the structure surrounding the pinch. The ESA is placed at 157 cm from the pinch. The fluxes measured at 157 cm are  $5.97 \times 10^7$  ions/cm<sup>2</sup> pinch for Xe<sup>+</sup>+Xe<sup>2+</sup>,  $3.7 \times 10^6$  ions/cm<sup>2</sup> pinch for W<sup>+</sup>, and  $8.3 \times 10^6$  ions/cm<sup>2</sup> pinch for Mo<sup>+</sup>. The total flux measured from Xe source, which includes all the ions (Xe<sup>+</sup>, Xe<sup>2+</sup>, W<sup>+</sup>, and Mo<sup>+</sup>) is  $7.17 \times 10^7$  ions/cm<sup>2</sup> pinch.

Ion debris is also measured from the SnCl<sub>4</sub>-fueled z pinch and is shown in Fig. 3. Several different ion species (Sn<sup>+</sup>, Sn<sup>2+</sup>, Mo<sup>+</sup>, Mo<sup>2+</sup>, W<sup>+</sup>, Cl<sup>+</sup>, Cl<sup>2+</sup>, C<sup>+</sup>, and N<sup>+</sup>) are resolved in this measurement. Sn<sup>+</sup>, Cl<sup>+</sup>, and N<sup>+</sup> ions are dominant species, whereas it is noticed that while both chlorine and nitrogen are significantly more abundant in the gas feed to the pinch area than Sn, there are more Sn ions measured at the ESA location than the other two species combined. It is possible that the chlorine and nitrogen ions underwent recombination more readily in the 157 cm between the pinch and the ESA, neutralizing their charge and making them invisible to the energy sector analyzer. This is supported by the fact that chlorine and nitrogen are lighter than tin and may be expelled from the pinch area with a lower initial charge. If this were the case, fewer recombinations during exposure would be necessary to enact this scenario.

The fluxes measured at 157 cm are  $1.06 \times 10^7$  ions/cm<sup>2</sup> pinch for Sn<sup>+</sup>+Sn<sup>2+</sup>,  $2.3 \times 10^4$  ions/cm<sup>2</sup> pinch for W<sup>+</sup>,  $1.03 \times 10^4$  ions/cm<sup>2</sup> pinch for Mo<sup>+</sup>+Mo<sup>2+</sup>,  $4.05 \times 10^6$  ions/cm<sup>2</sup> pinch for Cl<sup>+</sup>+Cl<sup>2+</sup>,  $1.5 \times 10^6$  ions/cm<sup>2</sup> pinch for N<sup>+</sup>, and  $4.35 \times 10^3$  ions/cm<sup>2</sup> pinch for C<sup>+</sup>. The total flux measured from the Sn source including all ions (Sn<sup>+</sup>, Sn<sup>2+</sup>, Mo<sup>+</sup>, Mo<sup>2+</sup>, W<sup>+</sup>, Cl<sup>+</sup>, Cl<sup>2+</sup>, C<sup>+</sup>, and N<sup>+</sup>) is 1.63

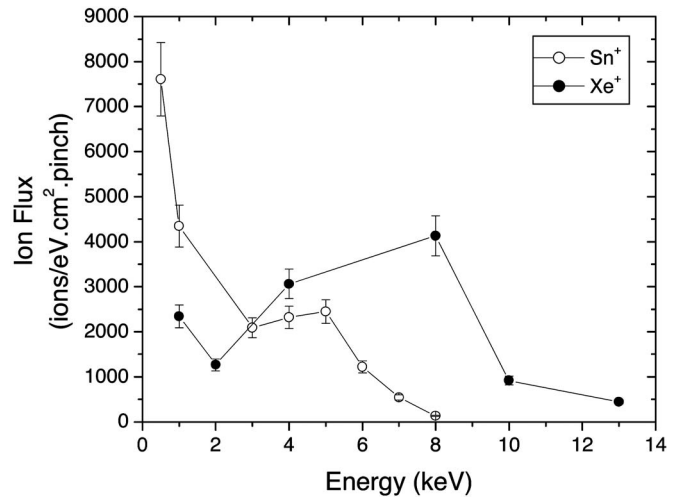


FIG. 4. Comparison of main fuel (Xe<sup>+</sup> and Sn<sup>+</sup>) produced in Xe and Sn sources.

$\times 10^7$  ions/cm<sup>2</sup> pinch. The singly charged fuel ions (largest overall abundance) have similar magnitudes, but all other ion species have lower magnitudes measured during Sn operation than during Xe operation. The exceptions to this are the Cl<sup>+</sup> and N<sup>+</sup> ions, which are uniquely present in the Sn pinch spectra due to the SnCl<sub>4</sub> delivery system (N<sub>2</sub> flows as a carrier gas). Due to the reduced flux of heavy ions, it is possible that EUVL collector optics would experience a longer lifetime with a Sn-fueled discharge-produced plasmas (DPP) than with a Xe-fueled DPP. It is not apparent, however, whether the effect of Sn condensation will make up this difference or even reduce EUV optics lifetime. This effect can be countered by strategies that remove Sn condensation from the mirrors or prevent its formation. It may therefore be possible to avoid these effects and take advantage of the increased EUV output available from the enhanced conversion efficiency of Sn and the decreased flux of heavy ions.

The relationship between the main fuel ion species (Sn<sup>+</sup>, Sn<sup>2+</sup>, Xe<sup>+</sup>, and Xe<sup>2+</sup>) are better shown in the direct comparison plots in Fig. 4. While Sn<sup>+</sup> ions have a larger flux at lower energies, the integrated flux is less than Xe<sup>+</sup>, since Xe<sup>+</sup> ions populate higher ionic energies. If we compare doubly ionized Xe and Sn ions, Xe<sup>2+</sup> is dominant (Fig. 5). Note the scales at

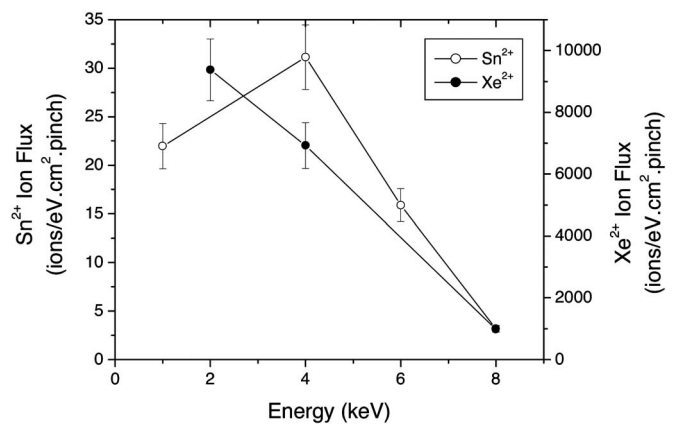


FIG. 5. Comparison of secondary fuel (Xe<sup>2+</sup> and Sn<sup>2+</sup>) produced in Xe and Sn sources.

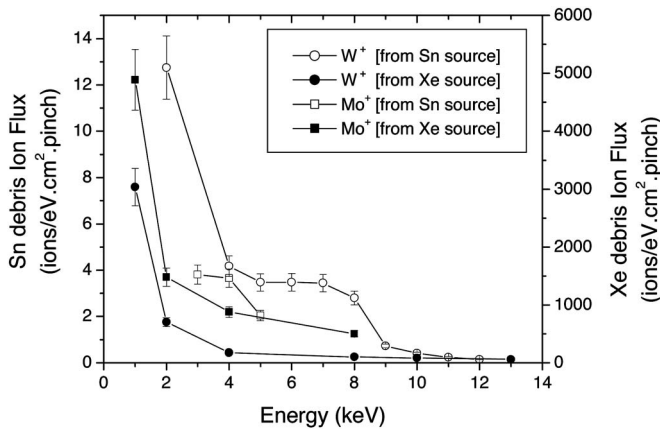


FIG. 6. Comparison of other ions produced in Xe and Sn sources.

left and right hand sides of the  $y$  axis.  $Xe^{2+}$  ion fluxes are over hundreds of orders of magnitude more than  $Sn^{2+}$  ions. A comparison of the ion fluxes of metal ions is shown in Fig. 6. While the singly charged fuel ion species ( $Sn^+$  and  $Xe^+$ ) are measured to have a similar flux (though a different energy peak), the other measured ions show smaller quantities from the  $SnCl_4$  pinch than the Xe pinch. The exceptions to this are the  $Cl^+$  and  $N^+$  ions seen from the Sn pinch. For the Xe source, the other debris fluxes are more than a factor of 500 times higher than debris fluxes obtained from the Sn sources.

Both DPPs and laser-produced plasmas (LPPs) create large electric fields that accelerate ions to very high energies<sup>6</sup> (8–15 keV). The implication is that high energy ions will bombard the collector optic surfaces and eventually damage them. Erosion, roughening, implantation, and deposition are potential mechanisms that can degrade mirror surfaces. Once the mirror surfaces are damaged, reflectivity decreases substantially. Mirror lifetime reductions result in frequent replacement, the end result of which is production downtime. This raises cost of ownership and is economically undesirable. Characterization of ion flux is critical to predicting these effects in a manufacturing setting. Other effects such as deposition and low energy debris can harm mirror surfaces, but these are minimal compared to the high erosive ion flux measured from these EUV sources.

In the case of Sn sources, mirror lifetime presents greater challenge. Apart from erosion due to high energetic ions, Sn also condenses and deposits on mirror surfaces. The EUV reflectivity in this case is affected by erosion as well as roughness caused by deposition. Additionally there are fast neutrals which contribute to erosive damage to the mirrors. Measured ion fluxes can be used to predict the mirror lifetime to a good approximation. These measurements are used below to validate the predicted erosion from models.

Several mirror samples are exposed to a Xe EUV source for  $10 \times 10^6$  pulses, and the erosion is measured using material characterization techniques such as scanning electron microscopy (SEM). Samples are exposed at normal incidence (C, Au, Mo, Si, and Si/Mo) and grazing incidence (Pd and Mo–Au) with respect to the pinch location ( $10^\circ$  for normal incidence and  $67^\circ$  for grazing incidence). Erosion is pre-

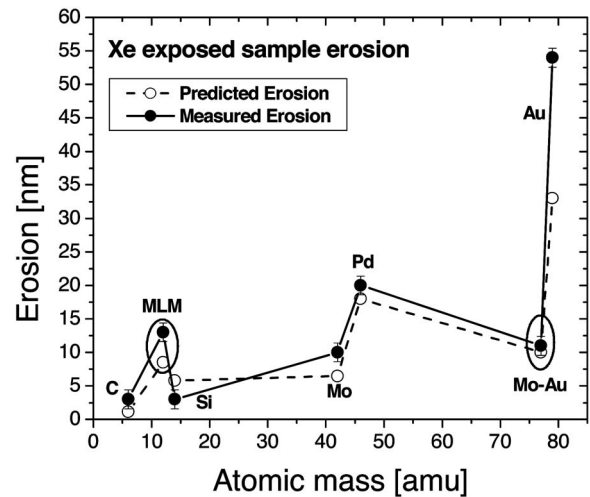


FIG. 7. Comparison of measured and predicted erosions for different materials.

dicted using the measured ion fluxes from the ESA in one case and the stopping and range of ions in matter (SRIM) code.

Erosion ( $\Delta T$ ) can be calculated, as shown in Eq. (1),

$$\Delta T = N \frac{m}{\rho} \text{ pulses}, \quad (1)$$

where  $m$  is the mass in grams,  $\rho$  is the density in  $g/cm^3$ , and  $N$  is the total eroded atoms.  $N$  is calculated from  $Y_{\text{Sputt}} \text{ion}_{\text{flux}}$ , where  $Y_{\text{Sputt}}$  is atoms sputtered per ion and  $\text{ion}_{\text{flux}}$  is the measured ion flux per  $cm^2$  per pulse.

Figure 7 shows the measured and predicted erosions for several materials investigated. It shows that measured and predicted values agree well. This good agreement suggests a possible application to accelerated lifetime testing. It should also be noted in Fig. 7 that predicted erosions are generally less than the measurements. We hypothesize that the neutral particles not taken into account by the ion fluxes used in Eq. (1), contribute to erosive damage of the collector optics. Measurement of neutral erosive flux is currently being pursued as part of the development of standardize diagnostic tool for debris measurement.

Similarly three different samples [Mo–Au, Ru, and multilayer mirror (MLM)] are exposed to the Sn source and analyzed. A photo of the MLM sample exposed to the Sn source is shown in Fig. 8. The surface appears thick and is covered with a gray contamination layer. An accurate measurement of erosion could not be obtained because of Sn deposition. However, rough values of erosion from SEM images are estimated as 20, 3, and 10 nm for Mo–Au, Ru, and MLM, respectively. Because of deposition problems, erosion on Sn exposed samples cannot be directly compared with Xe exposed samples. These deposition problems present a unique situation, where cleaning methods for the optics would be useful for successful realization of this technology. Qiu *et al.*<sup>24</sup> have performed a detailed investigation on Sn-exposed samples.

Mirror lifetime calculations are performed after verifying compatibility with experimental data to estimate limits

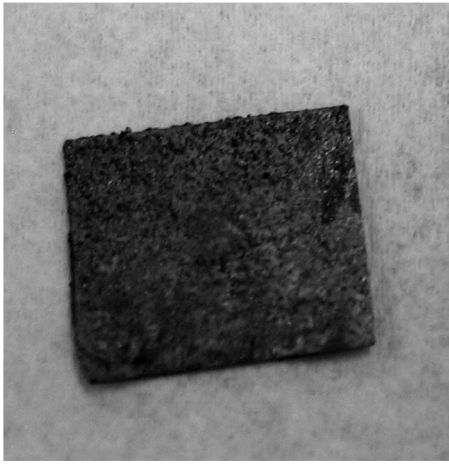


FIG. 8. Multilayer sample exposed to Sn-DPP EUV source, deposition from  $\text{SnCl}_4$  can be seen on the surface.

on collector lifetime for multilayer mirrors. Reflectivity degradation from collector optics is an effect of debris interaction with collector system. Two kinds of mirrors are used in extreme ultraviolet lithography, normal incidence mirrors (typically multilayer mirrors) and grazing incidence mirrors (typically homogeneous). For grazing incidence mirrors, roughness and contamination cause the reflectivity losses. In the case of normal incidence mirrors, in addition to roughness and contamination, erosion has a critical role to play in reflectivity degradation. MLMs are used as collector optics to generate extended lifetime against erosion from the source particle flux. As bilayers are eroded by the particle flux, sufficient underlying bilayers remain to maintain constant reflectivity. Calculations show (Fig. 9) how the reflectivity changes with number of bilayers eroded in a multilayer mirror. The highest reflectivity achieved using a MLM is around 73% (Fig. 9). We assume that the limit of reflectivity loss is 10% of the optimum value before the mirrors must be changed in a HVM setting. Calculations show that a minimum of 50 bilayers are needed to achieve the reflectivity at 73%, and erosion of 25 bilayers brings the reflectivity down to 10% of the optimum value.

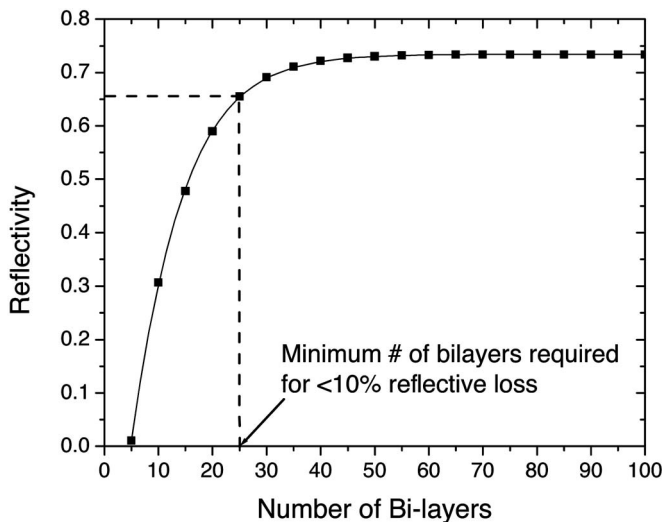


FIG. 9. Model calculation (reflectivity of multilayer mirrors as a function of the number of bilayers), a standard collector optics will have  $>50$  bilayers.

TABLE I. Basic material data for Ru, Si, and Mo.

MLM material	Standard thickness (nm)	Atomic mass (g)	Mass density ( $\text{g}/\text{cm}^3$ )
Ruthenium	1.50	$1.678 \times 10^{-22}$	12.3
Silicon	4.14	$4.664 \times 10^{-23}$	2.32
Molybdenum	2.76	$1.593 \times 10^{-22}$	10.2

It is important for source and mirror suppliers to be able to predict the number of pulses required to erode 25 bilayers of a multilayer mirror. The particle flux required to remove a given thickness of a substrate is

$$\Delta T_E = \frac{\Gamma_i Y_i t m_s}{\rho_s} + \frac{\Gamma_n Y_n t m_s}{\rho_s}, \quad (2)$$

where  $\Delta T$  is the change of thickness of the substrate due to erosion (cm),  $\Gamma$  is the particle flux ( $1/\text{cm}^2$  pulse),  $Y$  is the sputtering yield,  $t$  is the time of exposure (s),  $m$  is the substrate mass (g), and  $\rho$  is the substrate density ( $\text{g}/\text{cm}^3$ ). The subscripts  $i$  and  $n$  refer to ions and neutral particles, respectively.

Assuming that physical sputtering is the dominant erosion mechanism due to the low charge states reaching the mirror surface, the total sputtering yield is  $Y_i + Y_n = Y$  and the total particle flux is  $\Gamma_i + \Gamma_n = \Gamma$ . Therefore the total flux necessary to sputter away a layer of a given substrate is given by

$$\Gamma = \frac{\Delta T_E \rho_s}{Y t m_s}. \quad (3)$$

Table I shows material data (thickness in a multilayer mirror with a 1.5 nm thick capping layer of Ru, mass, and density) for Ru, Si, and Mo. Table II shows the sputtering yield of Ru, Si, and Mo using Xe and Sn at an average energy of 6 keV calculated using SRIM.

Using Eq. (3), the Xe fluence needed to remove an individual layer of Si or Mo is calculated to be  $6.17 \times 10^{15}$  particles/ $\text{cm}^2$  for Si and  $1.06 \times 10^{16}$  particles/ $\text{cm}^2$  for Mo. These values are tabulated in Table III. Thus the fluence required to remove one bilayer of Si/Mo is  $6.17 \times 10^{15} + 1.06 \times 10^{16} = 1.677 \times 10^{16}$  particles/ $\text{cm}^2$ . Multiplying this number by 25 bilayers gives the particle fluence required to produce a 10% reflectivity loss for a normal incidence mirror. This leads to calculation of the number of pulses required to erode 25 bilayers.

The experimental flux (from Xe source) measured using ESA at Illinois at 28 cm from the pinch location is  $1.87 \times 10^9$  ions/ $\text{cm}^2$  pinch, and the particle fluence required to erode one bilayer from MLM is  $1.677 \times 10^{16}$ . Therefore,  $1.87 \times 10^9 \times (\text{number of shots}) = 1.677 \times 10^{16}$ . This gives the number of shots required to erode one bilayer ( $\sim 9 \times 10^6$ ).

TABLE II. Sputtering yield calculation using SRIM from Ru, Si, and Mo.

MLM material	Xe (6 keV at $10^\circ$ )	Sn (6 keV at $10^\circ$ )
Ruthenium	4.38	4.65
Silicon	2.87	2.99
Molybdenum	1.94	1.93

TABLE III. Xe and Sn fluxes needed to erode one layer of Ru, Si, and Mo.

MLM material	Xe (6 keV at 10°)	Sn (6 keV at 10°)
Ruthenium	$2.34 \times 10^{15}$	$2.20 \times 10^{15}$
Silicon	$6.17 \times 10^{15}$	$5.93 \times 10^{15}$
Molybdenum	$1.06 \times 10^{16}$	$1.07 \times 10^{16}$

Therefore  $225 \times 10^6$  shots will erode 25 bilayers and reduce reflectivity by 10% of the original value. Based on this calculation, lifetime of multilayer collector mirrors is predicted. In HVM, if the source is operational at 10 kHz, the mirror lifetime is predicted to be only 6 h. This is unacceptable and demonstrates the need for effective debris mitigation systems. Characterizing ion flux with an ESA will allow comparison of the efficiency of different debris mitigation systems and prediction of collector optics lifetimes.

A similar calculation for Sn sources estimates the mirror lifetime to be 34 h. This is consistent with earlier measurements that Sn ion fluxes are less than Xe, allowing mirrors to survive longer in a Sn EUV source. As discussed above there are other factors that can damage collector optics in a Sn source. The contamination layer (Fig. 8) increases surface roughness, which would degrade reflectivity in addition to ion erosion. Therefore further characterization is required to determine which source actually maximizes collector lifetime.

In high volume manufacturing, the  $z$ -pinch source is operated at 10 kHz and expected mirror lifetime is targeted to  $1.1 \times 10^{11}$  pulses or about 3000 h.<sup>2</sup> Similarly in LPP EUV sources, the mirror lifetime for high volume manufacturing required is 1 yr or  $1.6 \times 10^{11}$  laser shots.<sup>13</sup> The lifetime calculation indicates the current status of EUV lithography. This calculation does not take into account available mitigation processes but does provide an estimate of degree of improvement required for specific EUV sources.

## SUMMARY

Extreme ultraviolet lithography has been chosen for for next generation lithography and will likely use Xe or Sn as an emitter. High energy ions released during dissipation of these plasmas are shown to degrade the lifetime of collector optics. This necessitates ion characterization and lifetime calculations at this phase of EUVL development. Ion fluxes and energy measurements are presented here in absolute units for Xe as well as Sn sources with a comparison of different ion species produced in these sources. Mirror samples are exposed to a Xe EUV source and erosion is measured using

SEM. Using the measured ion fluxes, erosion is predicted. SRIM calculations using measured ion flux are used to calculate expected erosion. This calculation agrees well with the measured erosion from sample exposures, but leaves room for energetic neutral contribution. Lifetime calculations are performed for Xe and Sn sources indicating the need for effective debris mitigation techniques.

## ACKNOWLEDGMENTS

We would like to express our thanks to Robert Bristol from Intel for his kind support and useful discussions and funding from INTEL SRA 03-159. We are thankful to XTREME GmbH, Germany for partially providing us the current EUV source and for their technical help from time to time as needed. We would also like to thank the Center for Microanalysis of Materials, University of Illinois. The results could not have been achieved without the help of our undergraduates John Sporre and Robert Lofgren.

<sup>1</sup>D. J. Resnick *et al.*, Proc. SPIE **6**, 205 (2002).

<sup>2</sup>*EUV Sources for Lithography*, edited by V. Bakshi (SPIE, Bellingham, WA, 2005).

<sup>3</sup>K. C. Thompson, E. Antonsen, M. R. Hendricks, B. E. Jurczyk, M. Williams, and D. N. Ruzic, Microelectron. Eng. **83**, 476 (2005).

<sup>4</sup>H. Komori, G. Soumagne, H. Hoshino, T. Abe, T. Saganuma, Y. Imai, A. Endo, and K. Toyoda, Proc. SPIE **5374**, 839 (2004).

<sup>5</sup>K. Takenoshita, C.-S. Koay, S. Teerawattanasook, and M. Richardson, Proc. SPIE **5374**, 954 (2004).

<sup>6</sup>D. N. Ruzic, K. C. Thompson, B. E. Jurczyk, E. Antonsen, S. N. Srivastava, and J. B. Spencer, IEEE Trans. Plasma Sci. **35**, 606–613 (2007).

<sup>7</sup>B. A. M. Hansson *et al.*, Rev. Sci. Instrum. **75**, 2122 (2004).

<sup>8</sup>K. Takenoshita, C.-S. Koay, S. George, S. Teerawattanasook, M. Richardson, and V. Bakshi, J. Vac. Sci. Technol. B **23**, 6 (2005).

<sup>9</sup>D. L. Rokusek, J. P. Allain, A. Hassanein, and M. Nieto, U.S. Department of Energy Journal of Undergraduate Research (<http://www.scied.science.doe.gov>).

<sup>10</sup>Martin Nieto *et al.*, J. Appl. Phys. **100**, 053510 (2006).

<sup>11</sup>M. Richardson, C.-S. Koay, K. Takenoshita, C. Keyser, and M. Al-Rabban, J. Vac. Sci. Technol. B **22**, 2 (2004).

<sup>12</sup>H. Komori *et al.*, J. Vac. Sci. Technol. B **21**, 6 (2003).

<sup>13</sup>B. A. M. Hansson *et al.*, Proc. SPIE **4688**, 102 (2002).

<sup>14</sup>R. J. Anderson, D. A. Buchenauer, L. Klebanoff, O. R. Wood II, and N. V. Edwards, Proc. SPIE **5374**, 710 (2004).

<sup>15</sup>XTREME Technologies GmbH, Göttingen, Germany ([www.xtremetec.de](http://www.xtremetec.de)).

<sup>16</sup>Osaka Vacuum, Ltd., Naniwa, Osaka, Japan ([www.osakavacuum.co.jp](http://www.osakavacuum.co.jp)).

<sup>17</sup>International Radiation Detectors, Inc., Torrance, CA ([www.ird-inc.com](http://www.ird-inc.com)).

<sup>18</sup>S. Bajt *et al.*, Proc. SPIE **7**, 236 (2003).

<sup>19</sup>Comstock, Inc., Oak Ridge, TN ([www.comstockinc.com](http://www.comstockinc.com)).

<sup>20</sup>Burle Electro-Optics, Sturbridge, MA ([www.burle.com](http://www.burle.com)).

<sup>21</sup>E. Antonsen, K. C. Thompson, M. R. Hendricks, D. A. Alman, B. E. Jurczyk, and D. N. Ruzic, J. Appl. Phys. **99**, 063301 (2006).

<sup>22</sup>Ortec®, Oak Ridge, TN ([www.ortec-online.com](http://www.ortec-online.com)).

<sup>23</sup>Agilent Technologies, Inc, Palo Alto, CA ([www.agilent.com](http://www.agilent.com)).

<sup>24</sup>H. Qiu, K. C. Thompson, S. N. Srivastava, E. L. Antonsen, D. A. Alman, B. E. Jurczyk, and D. N. Ruzic, J. Microolithogr., Microfabr., Microsyst. **5**, 033007 (2006).